Effect of Graphite Nanofibers on Poly(methyl methacrylate) Nanocomposites for Bipolar Plates

Min-Kang Seo and Soo-Jin Park*

*Dept. of Chemistry, Inha University, Incheon 402-751, Korea. *E-mail: sjpark@inha.ac.kr*
Received October 31, 2008, Accepted February 3, 2009

In this work, high-aspect-ratio graphite nanofibers (GNFs) were used to improve the electrical, thermal, and mechanical properties of the poly(methyl methacrylate) (PMMA) polymer, as well as those of PMMA composites suitable for use in bipolar plates. In the result, an electrical percolation threshold for the composites was formed between 1 and 2 wt% GNF content. This threshold was found to be influenced strongly by the three separate stages of the melt-blending process. The composites exhibited higher thermal and mechanical properties and lower thermal shrinkage compared with the neat PMMA. Thus, GNFs were demonstrated to have positive impacts on the thermo-mechanical properties of PMMA composites and showed, thereby, reasonable potential for use in composites employed in the fabrication of bipolar plates.

Key Words: Graphite nanofibers, Polymer, Composite materials, Thermal properties, Mechanical properties

Introduction

The polymer electrolyte membrane fuel cell (PEMFC) energy system can convert hydrogen and oxygen to electricity, leaving water as the only byproduct. not surprisingly then, this system is of great interest from an environmental point of view.[1-4] The most significant components of the PEMFC stack are the bipolar plates.[5,6] which account for about 80% of the total weight and 45% of the stack cost. They are designed for many functions, such as uniform distribution of reactants in active areas, heat removal from those areas, current carriage from cell to cell, and prevention of reactant and coolant leakages. The bipolar plates must also possess good thermal stability and low contact resistance.

The bipolar plates are a multi-functional component in a PEMFC stack. They provide the electrical connection from cell-to-cell and they separate the reactive gases. On the anode side of the plates, hydrogen gas is consumed to produce electrons and protons as follows:

$$2H_2 \rightarrow 4H^+ + 4e^- \quad (1)$$

The electrons are collected at the anode and the protons enter the electrolyte (oxidation of hydrogen). On the other side of the plates, i.e. at the cathode, oxygen gas combines with electrons from the cathode and protons from the electrolyte to produce water (reduction of oxygen) as follows:[7]

$$O_2 + 4H^- + 4e^- \rightarrow 2H_2O \quad (2)$$

In addition, the bipolar plates serve the following functions: (i) they facilitate water management with in the cell; (ii) they enable heat transfer; (iii) they support thin membranes and electrodes; (iv) they withstand the clamping forces of the stack assembly.[8] Therefore, the material requirements, such as in-plane electrical conductivity ($S \cdot cm^{-1}$), dimensional stability (%), flexural strength (MPa), tensile strength (MPa), impact strength (kgf·cm/cm), etc. should be satisfied for the construction of a bipolar plate.

Traditionally, the most commonly used bipolar plate material has been graphite. Among the advantages of graphite are excellent resistance to corrosion and low bulk resistivity. The disadvantages are its cost, difficulty in machining, and brittleness.[9,10] Given graphite's brittleness, the bipolar plate must be fabricated to a thickness on the order of several millimeters, which results in a voluminous and heavy fuelcell stack.[11] Metal is another good bipolar plate materials, offering the attributes of good electrical conductivity, low cost, excellent mechanical properties, and ease of fabrication. Metal is, however, unable to resist corrosion in fuel cells.[12,13]

Therefore, composite bipolar plates reinforced with graphite nanofibers (GNFs) are one of the promising alternatives to graphite, with its advantages of low cost, high conductivity, ease in machining, good corrosion resistance and low weight.[14-17]

In the present study, therefore, we prepared GNFs/poly(methyl methacrylate) (PMMA) composites in order to investigate the effect of GNF content on their thermal and mechanical properties and determine, thereby, the suitability of such composites for use in the bipolar plates.

Experimental

Materials. Vapor grown GNFs were supplied from Showa Denko Chem. Corporation. The GNFs had a low ash content (0.1 wt% or less), good elastic properties (young's modulus: 150~200 GPa, maximum tensile strength: 1~3 GPa), 50~150 nm diameter, and 50~100 μm length. The PMMA used in this study, obtained from Aldrich Chem. Co. had a melt flow index of 1.8 g/10 min (measured at 230 °C/3.8 kg).

Sample preparation. In preparation for composite production, the GNFs, as is commonly reported, were purified and functionalized to remove amorphous carbon and to open their highly tangled fibers.[18] PMMA was melt-blended with the addition of several GNF concentrations to the polymer: 1, 5, 10, and 15 wt%. The mixed samples were then compressed by hot press under a pressure of about 8 MPa at 220 °C for 10 min. GNFs/PMMA composite samples were obtained and

vacuum dried at 80 °C for 12 h before measurement.

Characterization and measurements. The room-temperature volume resistivity of the composites was measured using the four point-probe technique with parallel aluminum or platinum contacts according to ASTM method D257, using a resistivity test fixture and an electrometer. Product stoichiometries of the samples as functions of reaction temperature were obtained by thermogravimetric analysis (TGA, TA Instrument DMA 2980). All of the experiments were carried out under a nitrogen atmosphere at a purge rate of 50 mL/min. Dimensional changes of the composites under a heating rate of 5 °C/min and an applied stress of 0.2 MPa under N_2 gas were measured using a TA instrument thermo-mechanical analyzer (TMA 2940).

The mechanical properties of GNFs/PMMA composites are determined in terms of flexural strength, σ_f. The σ_f for the specimens determined from three-point bending test are calculated using the following equations:[19]

$$\sigma_f = \frac{3PL}{2bd^2} \tag{3}$$

where, P is the applied load, L the span length, b the width of specimen, d the thickness of specimen, ΔP the change in force in the linear portion of the load-deflection curve, and Δm the change in deflection corresponding to ΔP.

Impact strengths were obtained with a Tinius Olsel Model 66 Izod Impact Tester according to ASTM method D790.

Results and Discussion

Electrical properties. Figure 1 shows the volume resistivity of the GNFs/PMMA composites. For very low GNF contents, the resistivity gradually decreases with increasing GNF contents. However, at 5 wt%, a very definite reduction in resistivity is observed. This stepwise change in resistivity is a function of the formation of an interconnected GNF structure, and can be regarded as an electrical percolation threshold. This means simply that at contents between 1 and 5 wt% GNFs, a very high percentage of electrons are permitted to flow through the specimen due to the creation of an interconnecting conductive pathway. Considering the percolation threshold for three-dimensional (3D) systems, this low threshold value is likely to originate from filler materials with a 1D large aspect ratio, such as GNFs.[20]

Thermal properties. Figure 2 shows TGA thermograms of the GNFs/PMMA composites. The degradation onset temperatures can be calculated from the TGA curves by extrapolating, from the curve at the degradation peak, back to the initial weight of the polymer. Similarly, the end temperature of degradation can be calculated from the TGA curves by extrapolating from the curve at the degradation peak, forward to the final weight of the polymer. The composite specimen exhibits a degradation-onset temperature higher than that of pure PMMA. The peak degradation rates in the composites occur at about 40-60 °C above that in pristine PMMA. Therefore, the incorporation of high temperature nanoparticles, such as CNTs, leads to an increase of the thermal decomposition temperatures of composites.[21]

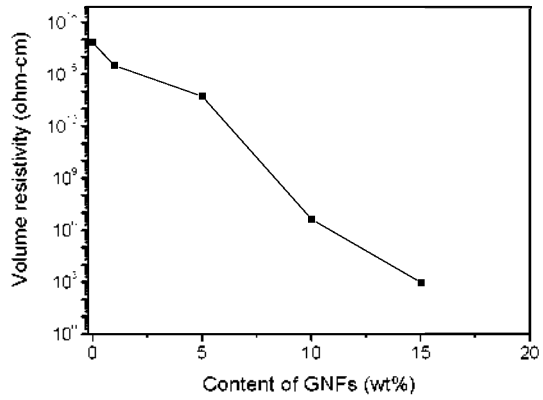

Figure 1. Electrical volume resistivity of GNFs/PMMA composites as measured by four-point probe method at room temperature.

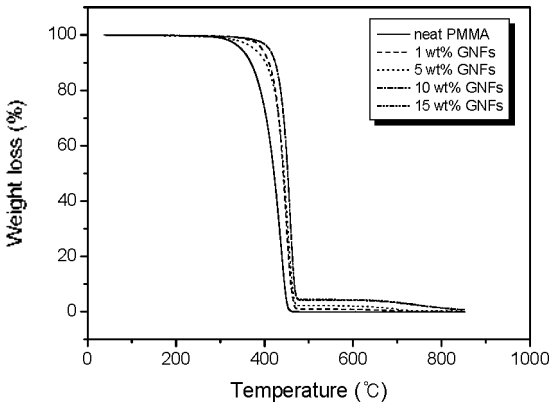

Figure 2. TGA curves of GNFs/PMMA composites as a function of GNF content.

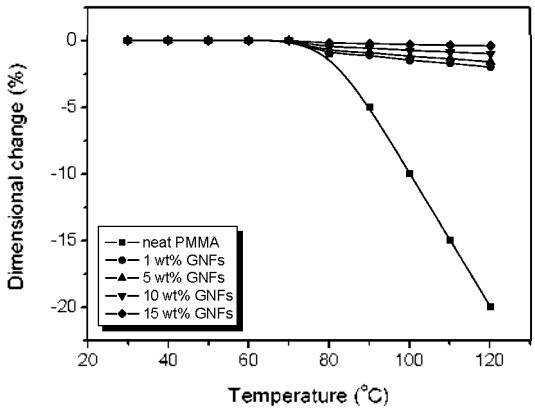

Figure 3. Dimensional change of GNFs/PMMA composites as a function of temperature.

Thermal shrinkage data for the GNFs/PMMA composites are given in Figure 3. Since PMMA is a glassy polymer, it is expected that considerable shrinkage would result when oriented fibers are allowed to relax at elevated temperatures.

This behavior is different from that observed when traditional semicrystalline polymer fibers, such as polyester and polypropylene, are exposed to elevated temperatures. The

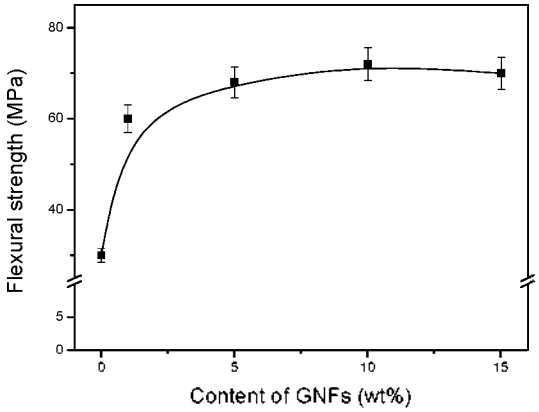

Figure 4. Flexural strength of GNFs/PMMA composites as a function of GNF content.

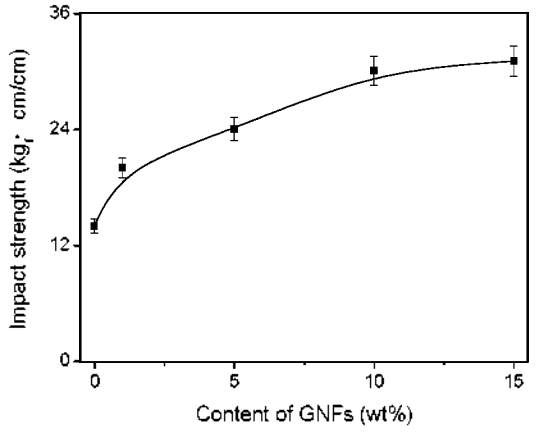

Figure 5. Impact strength of GNFs/PMMA composites as a function of GNF content.

absence of strain-induced crystallinity in PMMA leads to a large dimensional change (in Figure 3). However, the presence of GNFs decreases the magnitude of PMMA shrinkage considerably. At a temperature of approximately 110 °C, the pristine PMMA is found to shrink by 15%, whereas the composites, containing 2.5 wt% GNFs, exhibit only 5% shrinkage under the same conditions. One might also expect that the effect of reinforcement in glassy polymers, such as PMMA, would be more profound than would be observed in more rigid, semi-crystalline polymer composites.

Mechanical properties. Figure 4 shows the flexural strength of GNFs/PMMA composites as a function of GNF content. As reported in early, the flexural strength of the composite bipolar plates was primarily lower than the target value of 60 MPa.[22] However, the composite bipolar plates without GNFs had a flexural strength of 30 MPa, and the composite bipolar plates with GNFs had a flexural strength of 72 MPa. Consequently, it is found that the toughness of polymer-based composites can be improved by adding of GNFs. And they can form mesh-like structures to reinforce the materials due to the high aspect ratio of the nanofibers.[23] However, with increasing the GNF content, further improvement in mechanical properties of the composites cannot obtain because these are mainly determined by the dispersion state of GNFs in nano-fibers/matrix interfacial adhesion.

Figure 5 shows the impact strength of the GNFs/PMMA composites. The impact strengths are improved considerably by the inclusion of just 1-5 wt% GNFs and further improved with increasing GNF content, compared with the composites lacking GNFs. These results are owed to the fact that GNFs behave as crack arresters rather than (in most reinforced polymeric systems) crack initiators. PMMA and GNFs acting in a synergistic manner to yield that result.

GNFs-reinforced composites are much affected by impact-damage. In the course of an impact, the damaged zone, by means of matrix cracking, acts to magnify the stress locally. However, this impact-loading failure behavior is hindered by the GNFs' presence in the composites.[22-24] Thus, an increase in weight fraction of the composites improves the impact strength, minimally to 15 wt%, a fact also largely related to the fracture toughness of composites. In other words, the stronger is the interfacial adhesions, the higher is the impact strengths. Moreover, the fracture strain of carbon materials, such as GNFs and CNTs is estimated to be 10-30%, allowing for extensive bending, twisting, buckling, and reorienting, thereby imparting additional impact strength to the composites.

Conclusions

In this study we had clarified the role of GNFs on physico-chemical properties of their reinforced PMMA composites for bipolar plates. The glassy polymer, PMMA, was successfully reinforced by incorporation of GNFs *via* melt mixing. As a result, an electrical percolation threshold was formed between 1 and 5 wt% GNF contents. The GNFs/PMMA composites exhibited higher thermal and impact properties and lower thermal shrinkage compared with the pristine PMMA. Thus, GNFs were demonstrated to have a positive impact on the physicochemical properties of PMMA-based polymer composites, and showed a reasonable potential for use in composites employed in the fabrication of bipolar plates for PEMFC.

Acknowledgments. This work was supported by INHA UNIVERSITY Research Grant.

References

1. Steele, B. C. H.; Heinzel, A. *Nature* **2001**, *414*, 345.
2. Wagner, N. In *Electrochemical Power Sources-fuel Cells* in *Impedance Spectroscopy: Theory, Experiment, and Applications*, 2nd ed.; Barsoukov, E.; Ross Macdonald, J., Eds.; John Wiley & Sons: 2005; p 497.
3. Wagner, N.; Kaz, T.; Friedrich, K. A. *Electrochimica Acta* **2008**, *53*, 7475.
4. Larminie, J.; Dicks, A. In *Fuel Cell Systems Explained*; John Wiley & Sons: England, 2003.
5. Borup, R. L.; Vanderborgh, N. E. *Mater. Res. Soc. Symp. Proc.* **1995**, *393*, 151.
6. Hwang, I. U.; Yu, H. N.; Kim, S. S.; Lee, D. G.; Suh, J. D.; Lee, S. H.; Ahn, B. K.; Kim, S. H.; Lim, T. W. *J. Power Sources* **2008**, *184*, 90.
7. Wang, H.; Sweikart, M. A.; Turner, J. A. *J. Power Sources* **2003**, *115*, 243.

8. Du, L.; Jana, S. C. *J. Power Sources* **2007**, *172*, 734.
9. Larminie, J.; Dicks, A. In *Fuel Cell Systems Explained*; John Wiley & Sons: 2001.
10. Makkus, R. C.; Janssen, A. H. H.; Bruijn, F. A. de; Mallant, R. K. A. M. *Fuel Cells Bull.* **2000**, *17*, 5.
11. Wind, J.; Spah, R.; Kaiser, W.; Bohm, G. *J. Power Sources* **2002**, *105*, 256.
12. Davies, D. P.; Adcock, P. L.; Turpin, M.; Rowen, S. J. *J. Power Sources* **2000**, *86*, 237.
13. Tawfik, H.; Hung, Y.; Mahajan, D. *J. Power Sources* **2007**, *163*, 755.
14. Hammel, E.; Tang, X.; Trampert, M.; Schmitt, T.; Mauthner, K.; Eder, A. *Carbon* **2004**, *42*, 1153.
15. Seo, M. K.; Park, S. J. *Macromol. Mater. Eng.* **2004**, *289*, 368.
16. Seo, M. K.; Park, S. J.; Lee, S. K. *J. Colloid Interface Sci.* **2005**, *285*, 306.
17. Yang, J. H.; Kim, M. K.; Son, J. H.; Cho, H. J.; Kwon, Y. U. *Bull. Korean Chem. Soc.* **2007**, *28*, 1097.
18. Pötschke, P.; Bhattacharyya, A. R.; Janke, A. *Carbon* **2004**, *42*, 965.
19. Zhou, Y.; Pervin, F.; Lewis, L.; Jeelani, S. *Mater. Sci. Eng. A* **2008**, *475*, 157.
20. Moon, S. H.; Jin, W. J.; Kim, T. R.; Hahm, H. S.; Cho, B. W.; Kim, M. S. *J. Ind. Eng. Chem.* **2005**, *11*, 594.
21. Puglia, D.; Valentini, L.; Armentano, I.; Kenny, J. M. *Diamond Relat. Mater.* **2003**, *12*, 827.
22. Zhou, P.; Wu, C. W.; Ma, G. J. *J. Power Sources* **2007**, *163*, 874.
23. Choi, K. C.; Lee, E. K.; Choi, S. Y. *J. Ind. Eng. Chem.* **2004**, *10*, 402.
24. Park, S. J.; Jang, Y. S.; Rhee, K. Y. *J. Colloid Interface Sci.* **2002**, *245*, 383.